To be presented at the Thirteenth Symposium on Turbulence,
University of Missouri-Rolla, U.S.A, Sept. 21-23, 1992

DIFFERENTIAL DIFFUSION OF PASSIVE SCALARS IN STATIONARY ISOTROPIC TURBULENCE

P.K. Yeung † and S.B. Pope ‡

† School of Aerospace Engineering
Georgia Institute of Technology
Atlanta, GA 30332, U.S.A.

‡ Sibley School of Mechanical and Aerospace Engineering
Cornell University
Ithaca, NY 14853, U.S.A.

ABSTRACT

The differential diffusion of passive scalars of different diffusivities is studied by direct numerical simulations of statistically stationary isotropic turbulence at low Reynolds number. The statistical correlation between different scalars is closely linked to that between the gradients of different scalars. At small times the scalars de-correlate fairly rapidly, at a rate proportional to the square of the diffusivity difference. At large times the variance of each scalar decays exponentially in time at a slightly different rate, and the correlation coefficients continue to decrease, but only slowly. The question of whether the scalars ultimately become completely de-correlated (and remain so) requires further investigation.

INTRODUCTION

If two passive scalars of different molecular diffusivities are introduced into a turbulent flow and made identical-valued at some initial time instant, differing rates of diffusion cause them to subsequently become displaced and statistically de-correlated from each other. This phenomenon of differential diffusion has important effects on the structure of turbulent flames in which multiple diffusing species, including heat, of different diffusivities are almost always involved.

Most theoretical models of turbulent diffusion flames effectively ignore differential diffusion by assuming (a) the molecular diffusivities of all species, and of heat, to be equal, and (b) the effects of molecular diffusion to be negligible compared to turbulent diffusion. Assumption (a) is equivalent to taking the Lewis numbers of all species to be unity. These assumptions lead to great simplifications. However, Bilger and Dibble [1] pointed out that they are questionable at the low and moderate Reynolds numbers often encountered in turbulent flames. More recently, based on results reported by Chen *et al.* [2], Pope [3] noted that methods based on the equal-diffusivities assumption could not match experimental data.

As a basic fluid mechanics problem, the mixing of *multiple* scalars is not well understood, perhaps considerably less so than the mixing of a *single* scalar. For instance, there is little definite knowledge of the time scale on which two initially identical scalars de-correlate, and of whether the correlation coefficient between the two scalars attains a non-zero asymptotic value at large times. These are questions we address

in the present work.

We consider the differential diffusion between three passive scalars (taken in pairs) in numerically simulated isotropic turbulence. To provide a simplified setting in which to study the scalars, the hydrodynamic field is kept statistically stationary in time using the forcing scheme of Eswaran and Pope [4]. Direct numerical simulations are carried out using the pseudo-spectral algorithm of Rogallo [5] on a 64^3 grid. The time-averaged Taylor scale Reynolds number is 38, corresponding to one of the (hydrodynamic) simulations of Yeung and Pope [6]. Three initially Gaussian-distributed passive scalars ϕ_1, ϕ_2 and ϕ_3, at Schmidt numbers (Sc) 0.25, 0.5 and 1.0 respectively are introduced into the flow and allowed to evolve. High wavenumber spectra of the scalars are well resolved at these Schmidt numbers. After a transient period the decay of scalar variances becomes approximately exponential in time, consistent with the results of Eswaran and Pope [7]. Subsequently ϕ_1 and ϕ_2 are made identical to ϕ_3 (the scalar with unity Schmidt number). Differential diffusion effects become important in the ensuing evolution.

Our results show that the correlation coefficient decays rapidly at early times, but more slowly at later times. The small-time behavior is compared to an approximate analysis of the pure diffusion equation (with velocity field removed). The difference in diffusivities, rather than the ratios between them, is an important parameter. At large times the ensemble-averaged correlation coefficients appear to change slowly with no clear indication of approaching asymptotic values.

In the following sections, we give the basic equations governing differential diffusion, and an overview of the numerical simulations. Results are then presented for discussion. The path of further investigations is addressed.

BASIC EQUATIONS

Consider a set of σ passive scalars ϕ_1, $\phi_2, ..., \phi_\sigma$ evolving in a field of homogeneous isotropic turbulence. In the absence of mean scalar gradients, the mean value of each scalar may be taken to be zero without loss of generality. Then the fluctuation of each scalar ϕ_α ($\alpha = 1, ..., \sigma$, with no sum over Greek indices) evolves by the equation

$$\frac{\partial \phi_\alpha}{\partial t} + u_i \frac{\partial \phi_\alpha}{\partial x_i} = D_\alpha \frac{\partial^2 \phi_\alpha}{\partial x_i \partial x_i} , \tag{1}$$

where $u_i = u_i(\underline{x})$ is the fluctuating velocity field, and D_α is the diffusivity of the scalar ϕ_α. The diffusivity is constant but (in general) different for each scalar. As mixing proceeds, the scalar variance $\langle \phi_\alpha^2 \rangle$ decays according to

$$\frac{\partial \langle \phi_\alpha^2 \rangle}{\partial t} = -2D_\alpha \left\langle \left(\frac{\partial \phi_\alpha}{\partial x_i} \right)^2 \right\rangle \equiv -\chi_\alpha , \tag{2}$$

where χ_α is the dissipation rate of the scalar ϕ_α.

In studies of differential diffusion the covariance of two scalars, $\langle \phi_\alpha \phi_\beta \rangle$, is important. It evolves by

$$\frac{\partial \langle \phi_\alpha \phi_\beta \rangle}{\partial t} = -(D_\alpha + D_\beta) \left\langle \frac{\partial \phi_\alpha}{\partial x_i} \frac{\partial \phi_\beta}{\partial x_i} \right\rangle \equiv -\chi_{\alpha\beta}, \tag{3}$$

where $\chi_{\alpha\beta}$ denotes the "joint" dissipation. (Unlike χ_α, when $\alpha \neq \beta$, $\chi_{\alpha\beta}$ is not necessarily positive.) From Eqs. 2 and 3 it may be shown that the cross-correlation coefficient between the scalars ϕ_α and ϕ_β, i.e.,

$$\rho_{\alpha\beta} \equiv \frac{\langle \phi_\alpha \phi_\beta \rangle}{[\langle \phi_\alpha^2 \rangle \langle \phi_\beta^2 \rangle]^{1/2}} ,$$

evolves by

$$\frac{\partial \rho_{\alpha\beta}}{\partial t} = [\langle \phi_\alpha^2 \rangle \langle \phi_\beta^2 \rangle]^{-3/2} [-\langle \phi_\alpha^2 \rangle \langle \phi_\beta^2 \rangle \chi_{\alpha\beta} + \frac{1}{2} \langle \phi_\alpha \phi_\beta \rangle (\langle \phi_\alpha^2 \rangle \chi_\beta + \langle \phi_\beta^2 \rangle \chi_\alpha)] . \tag{4}$$

Equation 4 may be viewed as a "budget" equation for the two-scalar cross-correlation coefficient. This equation directly confirms two qualitative expectations. First, consider that the two scalars be made identical valued at some initial instant t_0. Since the scalar fluctuations are differentiable in time, a simple Taylor expansion shows that the correlation coefficient must depart from unity quadratically in time. Consistent with this fact, Eq. 4 indicates that $\partial \rho_{\alpha\beta}/\partial t = 0$ at $t = t_0$. The second expectation is that if the variances of both scalars as well as the their covariance decay exponentially with time at the *same* rate, then their cross-correlation coefficient does not change. In this case $\langle \phi_\alpha^2 \rangle$, $\langle \phi_\beta^2 \rangle$ and $\langle \phi_\alpha \phi_\beta \rangle$ are all proportional to $\exp(-ct)$, where c is some positive constant. Substituting the corresponding forms for the dissipations (via Eqs. 2 and 3) in Eq. 4 again leads to a vanishing time derivative for the two-scalar correlation coefficient.

Clearly, the correlation between the *gradients* of two scalars, through the joint dissipation, plays an important role. In the results section, we study the dynamics of the correlation between pairs of scalars and between their gradients with reference to the equations presented above.

OVERVIEW OF SIMULATIONS

The exact Navier-Stokes equations are solved together with the scalar transport equation (1) numerically to obtain velocity and scalar fluctuations. This is accomplished by carrying out direct numerical simulations (DNS) of homogeneous isotropic turbulence using the Fourier pseudo-spectral algorithm of Rogallo [5] in the form implemented by Yeung and Pope [8]. The solution domain is a 64^3 uniform grid with periodic boundary conditions imposed in three dimensions. The hydrodynamic field is made statistically stationary in time using the forcing scheme of Eswaran and Pope [4]. The time-averaged Taylor-scale Reynolds number is 38, with all hydrodynamic statistics corresponding closely to those of the first-listed simulation in Yeung and Pope [6]. (In effect, numerical parameters are chosen to obtain different realizations of statistically the same flow.)

The scalars are introduced first using Gaussian distributed random numbers in conjunction with a specified wavenumber spectrum. This Gaussian state is unphysical because it implies Gaussian distributed scalar gradients as well. However, when the scalar is allowed to evolve, after a transient period it attains a self-similar state, independent of the details of the initial spectrum. Self-similarity of the scalar is characterized by approximate exponential decay of variance with time, a Gaussian probability density function (p.d.f.) for the scalar but not for the gradients, and a collapse of the high-wavenumber scalar spectrum under Kolmogorov scaling. The case of $Sc = 1$ is taken as reference, and after it has remained self-similar for a few eddy-turnover times, two other scalars at $Sc = 0.25$ and $Sc = 0.5$ are introduced and made identical-valued to the $Sc = 1$ scalar. We choose Schmidt number values not exceeding unity so that, like the hydrodynamic field, the scalar fields remain well-resolved at the small scales. The drawback is that for small Schmidt numbers (say 0.25)

the scalar spectrum quickly becomes dominated by the large scales. This contributes to statistical variability since relatively few samples of the large-scale modes exist in the solution domain.

Unlike the forced hydrodynamic field, the scalar fields are not statistically stationary and thus time averages are not taken. Consequently, each run represents only one realization, and considerable differences between realizations can be expected. Indeed, the numerical results presented in this paper exhibit significant statistical variability, especially at long diffusion times. This necessitates performing ensemble averaging over multiple independent realizations that are statistically identical but different in detail. Different realizations are created by introducing randomness via the initial conditions, and via the forcing scheme which is based on a stochastic process. Since each simulation covered as long as 16 eddy-turnover times, the velocity and scalar fields at the beginning and end may be considered statistically independent. Thus, the final conditions for each run are conveniently taken to be the initial conditions for the next run, with each run then representing a different realization. We have obtained and processed 11 realizations in this manner. For the forcing scheme, since only a small number of large scale modes are forced, insufficient sampling of the forced modes leads to large temporal fluctuations in volume-averaged flow statistics, as previously discussed by Yeung and Pope [6].

Differential diffusion occurs when the three scalars of different diffusivities are subsequently allowed to evolve together. Results are presented in the next few sections. For convenience, time is measured from the instant at which the scalars are made identical, and the scalar variances at this time (called *initial* time hereafter in this article) are normalized to unity.

RESULTS AND DISCUSSION

In this section, we describe and discuss the temporal evolution of scalar variances, covariances and cross-correlation coefficients. The behavior at small and large times are separately discussed further. In view of the statistical variability at (especially) large diffusion times, ensemble averaging is performed over multiple realizations created in the manner described in the previous section.

Figure 1 shows the evolution of scalar variances and covariances, which are equal at the initial time at which the scalar fluctuations are made identical valued. The dissipation of scalar fluctuations by mixing occurs faster for more strongly diffusing scalars with lower Schmidt numbers. A transient period necessarily occurs during which the scalars adjust to the different rates of mixing. At large times the data suggest exponential decay of the variances in time, represented by approximately straight lines of constant slopes on the linear-log plot. Exponential decay at large times was also observed in forced stationary turbulence by Eswaran and Pope [7] who used very different initial conditions for the scalars.

True exponential decay of the variance implies a constant decay time scale, defined as the ratio of variance to dissipation. Eswararn and Pope [7] used only one Schmidt number of 0.7. To compare the decay time scales of different scalars of different Schmidt numbers among themselves and to that of the velocity field, we show in Fig. 2 the evolution of the mechanical-to-scalar time scale ratios

$$r_\alpha = (q^2/\langle\varepsilon\rangle)\,(\chi_\alpha/\langle\phi_\alpha^2\rangle)\ .$$

(Here $q^2/2$ and $\langle\varepsilon\rangle$ are the mean turbulence kinetic energy and dissipation rate respectively.) Except during

an initial transient period, the time scale ratio r_α oscillates around a value slightly greater than 5, which is qualitatively consistent with the results of Eswaran and Pope [7] (in which the definition of scalar dissipation was half of that used in this paper). However, a slight but systematic dependence of the decay time scale on Schmidt number can be discerned. Lower Schmidt number is seen to be associated with a larger mechanical-to-scalar time scale ratio, and hence a smaller decay time scale and larger decay rate for the scalar variance.

The transient period observed in Fig. 2 appears to be less than one eddy-turnover time. Concurrently, the spectra of the two initially-perturbed scalars ($Sc = 0.25$ and 0.5) are found to adjust rapidly to a statistically steady shape under Kolmogorov scaling. Figure 3 shows the scaled steady-state spectra for all three scalars, using the the same scaling as Kerr [9]. The spectra are well resolved, with small or no turn-up at the high wavenumber end. The spectral collapse at later times is consistent with self-similar decay of each scalar. The p.d.f. of each scalar remains near-Gaussian throughout the simulations. We also observe that, as expected, the spectra of scalars of lower Schmidt numbers have more low wavenumber content.

Figure 4 shows the correlation coefficient between the $Sc = 0.25$ and $Sc = 1$ scalars for 11 different realizations, up to 16 eddy-turnover times. This pair of scalars has the largest diffusivity difference among the three scalars used. The sample mean and standard deviation are also indicated. It may be seen that at early times (less than one eddy-turnover time) the correlation coefficient decreases fairly rapidly with little statistical uncertainty. In contrast, the different realizations differ widely at later times. The possibility of asymptotic values at large times is explored further at the end of this section.

The correlation coefficients of all three pairs of scalars are compared in Fig. 5. Besides the sample means, 90% confidence intervals for the ensemble averages are also indicated. (That is, at each given time the ensemble-averaged correlation coefficient falls inside the marked intervals with 90% probability.) Differential diffusion between the $Sc = 0.25$ and $Sc = 1$ scalars is clearly much more pronounced than for the other two pairs. The pairs $Sc = 0.25, 0.5$ and $Sc = 0.5, 1.0$ share the same diffusivity ratio. However, the correlation coefficient is consistently lower for the *former*—i.e., the pair with higher diffusivities and larger diffusivity differences.

According to Eq. 3, the rate of de-correlation of scalar fluctuations is tied to the de-correlation of the gradients of different scalars. Figure 6 shows the evolution of the scalar-gradient correlation coefficients $g_{\alpha\beta}$ (defined similarly to $\rho_{\alpha\beta}$) averaged over different realizations and (in view of isotropy) over different coordinate components. Clearly, the scalar gradients are persistently more strongly de-correlated than the scalars themselves. Statistical variability, as measured by the size of the confidence intervals, is substantially less than that for the scalars. Since the gradients are more closely related to the small scales, this comparison is consistent with the expectation that the statistical uncertainty arises mainly at the large scales. At large times the correlation coefficient between the scalar gradients appears to approach a quasi-steady value, or at least changes very slowly.

Small-time behavior

At sufficiently small times it is natural to expect differential diffusion to be largely determined by the small scales (which have the shortest time scales) at which molecular effects are most important. Thus

an approximate analysis can be made based on the pure diffusion equation, (Eq. 1 with the advective term removed)

$$\frac{\partial \phi_\alpha}{\partial t} = D_\alpha \nabla^2 \phi_\alpha \ . \tag{5}$$

Let $\hat{\phi}_\alpha(\underline{k},t)$ be the Fourier transform of the scalar field $\phi_\alpha(\underline{x},t)$, where $\underline{k}$ is the wave-vector with magnitude k. The Fourier-space equivalent of Eq. 5 is

$$\frac{\partial \hat{\phi}_\alpha}{\partial t} = -D_\alpha k^2 \hat{\phi}_\alpha \ , \tag{6}$$

which upon integration gives

$$\hat{\phi}_\alpha(\underline{k},t) = \hat{\phi}_0(\underline{k}) \exp(-D_\alpha k^2 t) \ , \tag{7}$$

where the subscript '0' denotes initial conditions which are identical for all scalars. The scalar spectrum is given by

$$E_{\alpha\alpha}(\underline{k},t) = \langle \hat{\phi}_\alpha \hat{\phi}_\alpha^* \rangle = E_0(\underline{k}) \exp(-2D_\alpha k^2 t) \ , \tag{8}$$

and so the variance can be expressed as

$$\langle \phi_\alpha^2 \rangle = \int E_0(\underline{k}) \exp(-2D_\alpha k^2 t) d\underline{k} \ , \tag{9}$$

where the integral is taken over all Fourier modes. Similarly, the covariance is given by

$$\langle \phi_\alpha \phi_\beta \rangle = \int E_0(\underline{k}) \exp[-(D_\alpha + D_\beta) k^2 t] d\underline{k} \ . \tag{10}$$

The correlation coefficient is hence

$$\rho_{\alpha\beta} = \frac{\int E_0(\underline{k}) e^{-(D_\alpha + D_\beta)k^2 t} d\underline{k}}{\{\int E_0(\underline{k}) e^{-2D_\alpha k^2 t} d\underline{k} \int E_0(\underline{k}) e^{-2D_\alpha k^2 t} d\underline{k}\}^{1/2}} \ . \tag{11}$$

By expanding the exponentials, $\langle \phi_\alpha \phi_\beta \rangle$ can be written in terms of even moments of the initial scalar spectrum:

$$I_p = \int E_0(\underline{k}) k^p d\underline{k} \ , \tag{12}$$

where $p = 0, 2, 4, ...$, and I_0 is just the initial variance.

Consider now times so small that Eq. 11 can be expanded as a binomial series, with higher order terms neglected. After straightforward algebra, the final result is:

$$\rho_{\alpha\beta}(t) = 1 - \frac{1}{2}(D_\alpha - D_\beta)^2 [I_4/I_0 - (I_2/I_0)^2] t^2 + O(t^4) \ . \tag{13}$$

The factor $I_4/I_0 - (I_2/I_0)^2$ depends on the shape of the initial scalar spectrum. In general, $I_4/I_0 > (I_2/I_0)^2$, so that $\rho_{\alpha\beta}(t)$ initially decreases quadratically with time. This analysis also shows that, at least initially, the rate of de-correlation is proportional to the square of the diffusivity difference. The result (13) is compared to numerical data in Fig. 7. To accentuate the quadratic behavior, we have plotted $1 - \rho_{\alpha\beta}(t)$ versus time on log-log-scales. Since the early time evolution is a small scale process, time is normalized by the Kolmogorov time scale (which is 0.136 T_E in this flow). The agreement is evidently close at sufficiently small diffusion times. Also, the range of validity of (13) is longer for lower Schmidt numbers at which the diffusive effects are stronger compared to the convective effects.

Large-time behavior

There is natural interest in whether the scalar and scalar-gradient correlation coefficients approach zero, representing complete de-correlation, or other asymptotic value at long enough diffusion times. Figures 5 and 6 indicate that asymptotic values, if they do occur, are not yet reached after 16 eddy-turnover times. Within the limits of statistical uncertainty, the correlation coefficients show a continuing but slow trend of approximately linear decrease with time. If the ensemble-averaged joint-scalar correlation coefficients are extrapolated linearly in time, they would reach zero at nearly 45 eddy-turnover times for the $Sc = 0.25$ and 1.0 pair, and as long as 160 eddy-turnover times for the $Sc = 0.5$ and 1.0 pair.

The question of long-time asymptotic behavior can be addressed further using Eq. 4. The rate of change of the joint-scalar correlation coefficient is determined by two competing effects. A positive joint-scalar correlation coefficient tends to reinforce itself, while a positive correlation of the scalar gradients tends to de-correlate the scalars. The relative magnitudes of these effects are compared in Fig. 8, where they are seen to nearly balance. The overall rate of change is indeed small—on average, for the $Sc = 0.25$ and 1.0 scalars, it takes some 5 eddy-turnover times for the correlation coefficient to decrease by 0.1. (For comparison, according to Fig. 1, in the same time interval the scalar variances decay by a factor of of order at least 10^3.)

We earlier remarked that if the scalar variances and covariances all decay at the same rate, the correlation coefficients would become constant. However, the decay time scales are seen in Fig. 2 to be different for each scalar. Considering also the trends observed in Fig. 5 and 6, it seems more likely that, on average, the correlation coefficients would continue to decrease. Nevertheless, this statement needs to be tested by further numerical simulations over extended periods of time. We may note that if the scalars and their gradients become perfectly uncorrelated at some time, then Eq. 4 indicates that the correlation coefficients would pass through another inflection point at which the first-order time derivative $\partial\rho_{\alpha\beta}/\partial t$ vanishes. Additional interesting deductions may be drawn from Eq. 4, but will be reported elsewhere.

CONCLUSIONS AND FURTHER WORK

We have studied the differential diffusion of passive scalars with different diffusivities, a problem especially important in turbulent combustion, in the case of statistically stationary isotropic turbulence. The dimensionless parameters are a Taylor-scale Reynolds number of 38, and Schmidt numbers of 0.25, 0.5 and 1.0.

It is shown that each scalar attains a self-similar state and decays exponentially in time with a slightly different decay time scale. The scalars are initially identical but subsequently de-correlate due to differential diffusion. At small diffusion times the joint-scalar correlation coefficient departs from unity quadratically in time, proportionally to the square of the diffusivity difference, and to a parameter describing the shape of the scalar spectrum.

At large diffusion times the data show considerable statistical variability among different realizations. The ensemble-averaged correlation coefficients between different scalars and between the gradients of different scalars appear to decrease slowly up to 16 eddy-turnover times and beyond. A definitive answer to the question

of long-time asymptotic behavior awaits further investigations.

This work will be extended in several directions. The numerical simulations will be extended to cover longer diffusion times. Whereas this paper is largely based on statistical analysis in physical space, useful insights may also be gained using Fourier-space descriptions and three-dimensional visualization. The effects of Reynolds number, and of different types of initial conditions are also to be studied.

REFERENCES

[1] R.W. Bilger and R.W. Dibble, "Differential molecular diffusion effects in turbulent mixing," Comb. Sci. & Tech. **28**,161 (1982).

[2] J-Y. Chen, R.W. Bilger and R.W. Dibble, "PDF modeling of turbulent nonpremixed $CO/H_2/N_2$ jet flames with reduced mechanisms," Twenty-Third Symposium (International) on Combustion, The Combustion Institute, 775 (1990).

[3] S.B. Pope, "Computations of turbulent combustion: progress and challenges," Twenty-Third Symposium (International) on Combustion, The Combustion Institute, 591 (1990).

[4] V. Eswaran and S.B. Pope, "An examination of forcing in direct numerical simulations of turbulence," Comput. & Fluids **16**, 257 (1988).

[5] R.S. Rogallo, "Numerical experiments in homogeneous turbulence," NASA TM 81315 (1981).

[6] P.K. Yeung and S.B. Pope, "Lagrangian statistics from direct numerical simulations of isotropic turbulence," J. Fluid Mech. **207**, 531 (1989).

[7] V. Eswaran and S.B. Pope, "Direct numerical simulations of the turbulent mixing of a passive scalar," Phys. Fluids **31**, 506 (1988).

[8] P.K. Yeung and S.B. Pope, "An Algorithm for tracking fluid particles in numerical simulations of homogeneous turbulence," J. Comput. Phys. **79**, 373 (1988).

[9] R.M. Kerr, "Higher-order derivative correlations and the alignment of small-scale structures in isotropic numerical turbulence," J. Fluid Mech. **153**, 31 (1985).

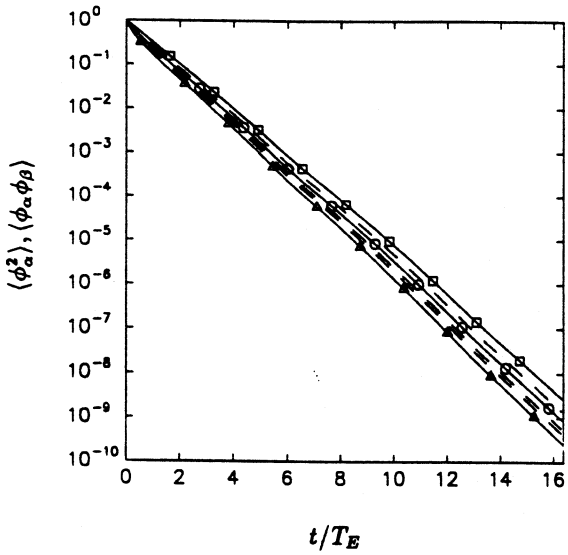

Fig. 1. The decay of variances and covariances with time normalized by the eddy-turnover time (T_E, the ratio of longitudinal integral length scale to the root-mean-square velocity). Schmidt numbers for variances are: 0.25 (ϕ_1, △), 0.5 (ϕ_2, ○) and 1.0 (ϕ_3, □). Covariances are shown as dashed lines, with $\langle\phi_2\phi_3\rangle > \langle\phi_1\phi_3\rangle > \langle\phi_1\phi_2\rangle$ at all times.

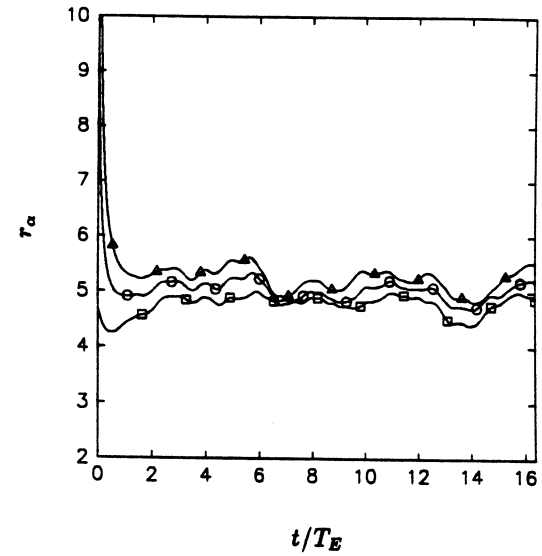

Fig. 2. Evolution of the mechanical-to-scalar time scale ratio r_α for the three scalars, shown in normalized time. Schmidt numbers are: 0.25 (△), 0.5 (○) and 1.0 (□).

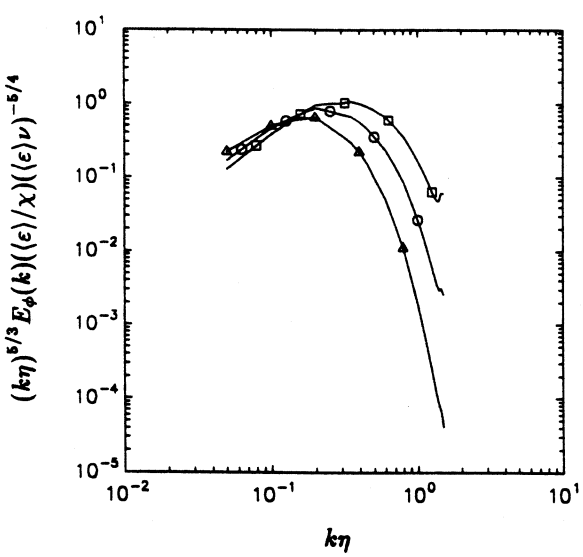

Fig. 3. Three-dimensional scalar spectra ($E_\phi(k)$) in the self-similar period of decay, shown in Kolmogorov scaling (ν is the kinematic viscosity, and η is the Kolmogorov length scale). Schmidt numbers are: 0.25 (△), 0.5 (○) and 1.0 (□).

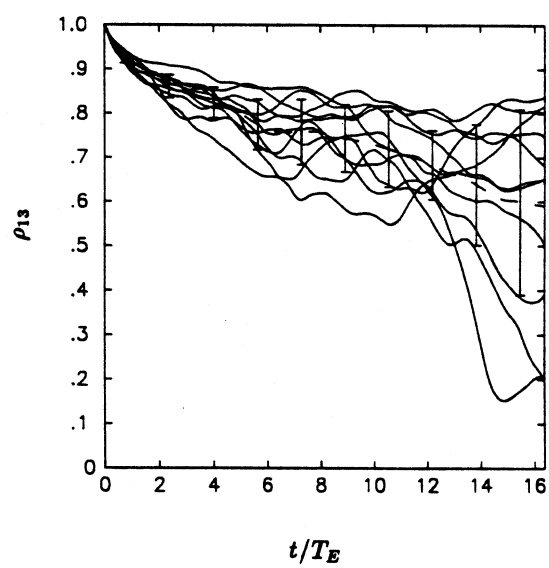

Fig. 4. Evolution of the correlation coefficients between the $Sc = 0.25$ (ϕ_1) and $Sc = 1$ (ϕ_3) scalars shown in normalized time. Each solid line represents a different realization. The dashed line represents the average over all (11) realizations, and the vertical bars indicate one standard deviation above and below the mean.

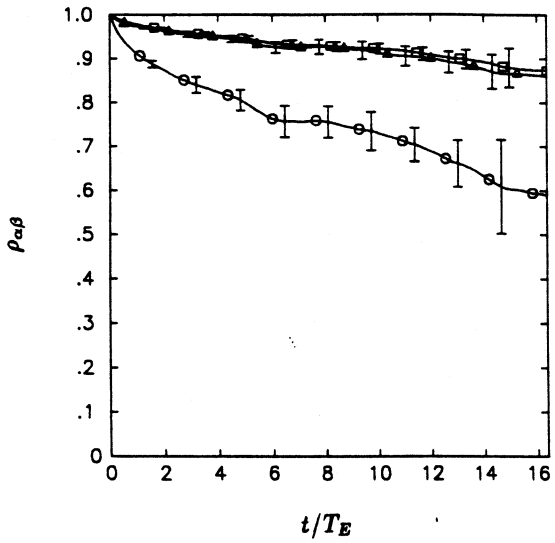

Fig. 5. Evolution of the correlation coefficients between different scalars taken in pairs: $Sc = (0.25, 0.5)$ ($\triangle$), $Sc = (0.25, 1.0)$ ($\bigcirc$), and $Sc = (0.5, 1.0)$ ($\square$), shown in normalized time. The lines shown are averages over multiple realizations. Vertical bars denote bounds of 90% confidence intervals (calculated using Student's t distribution because sample size is small) for the respective ensemble averages.

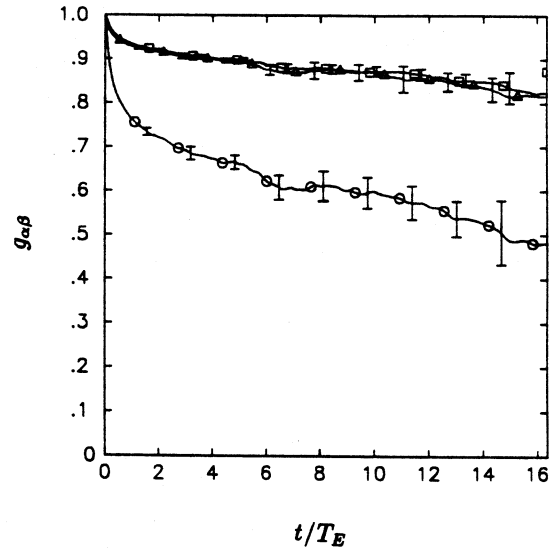

Fig. 6. Same as Fig. 5, but for correlation coefficients between the gradients of the different scalars.

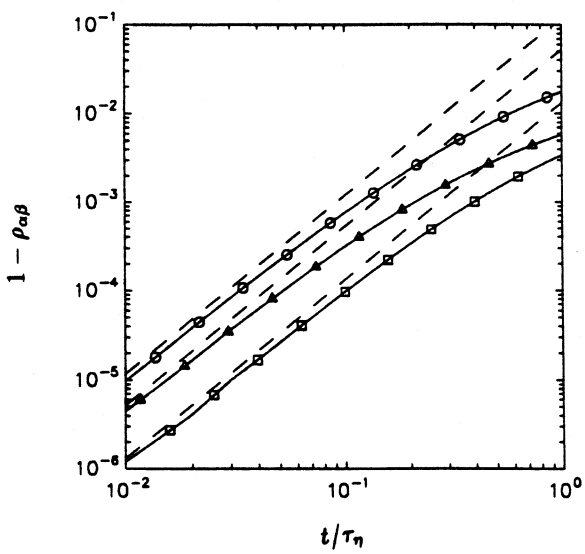

Fig. 7. Comparison of the evolution of two-scalar correlation coefficients at very small diffusion times (normalized by the Kolmogorov time scale τ_η) with prediction from analysis of the diffusion equation (Eq. 13). The scalar pairs are: $Sc = (0.25, 0.5)$ ($\triangle$), $Sc = (0.25, 1.0)$ ($\bigcirc$), and $Sc = (0.5, 1.0)$ ($\square$).

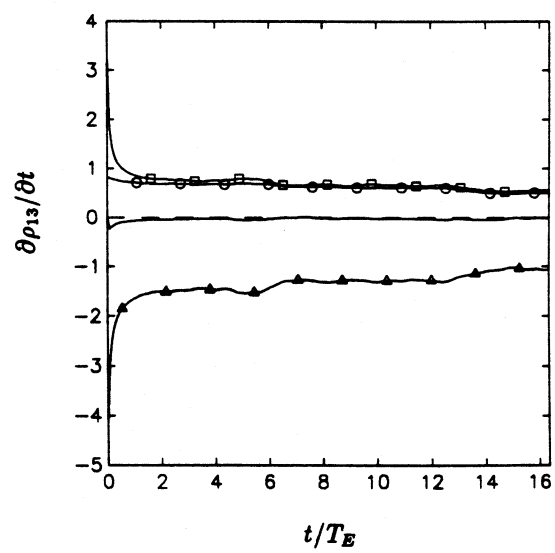

Fig. 8. Breakdown of the rate of change of the correlation coefficient (un-marked solid line) between the $Sc = 0.25$ (ϕ_1) and 1.0 (ϕ_3) scalars into three terms according to Eq. 4: $-\langle\phi_1^2\rangle\langle\phi_3^2\rangle\chi_{13}$ ($\triangle$), $\frac{1}{2}\langle\phi_1\phi_3\rangle\langle\phi_1^2\rangle\chi_3$ ($\bigcirc$), and $\frac{1}{2}\langle\phi_1\phi_3\rangle\langle\phi_3^2\rangle\chi_1$ ($\square$), all normalized by $[\langle\phi_1^2\rangle\langle\phi_3^2\rangle]^{3/2}$.